ChemPhysChem

Research Article
doi.org/10.1002/cphc.202200154

Chemistry Europe
European Chemical
Societies Publishing

www.chemphyschem.org

Chasing Self-Assembly of Thioether-Substituted Flavylium Salts in Solution and Bulk State

Julius A. Knöller,[a] Robert Forschner,[a] Wolfgang Frey,[a] Johannes Lang,[a] Angelika Baro,[a] Anna Zens,[a] Yann Molard,[b] Frank Giesselmann,[c] Birgit Claasen,[a] and Sabine Laschat*[a]

Dedicated to Professor Herbert Mayr on the occasion of his 75th birthday

Two series of flavylium triflates carrying alkoxy side chains in the A-ring (benzo unit of chromylium salt) and thioethers in the B ring (phenyl unit) (O_n-**Fla**-S_m) as well as thioethers at both A and B ring (S_n-**Fla**-S_m) were synthesized in order to understand the effect of thioether functionalization on their self-assembly and electronic properties. Concentration-dependent and diffusion ordered (DOSY) NMR experiments of O_1-**iV**-**Fla**-S_3 indicate the formation of columnar H-aggregates in solution with antiparallel intracolumnar stacking of the AC unit (chromylium) of the flavylium triflate, in agreement with the solid state structure of O_1-**V**-**Fla**-S_1. Thioether substitution on the B ring changes the linear optical properties in solution, whereas it has no effect on the A ring. According to differential scanning calorimetry, polarizing optical microscopy and X-ray diffraction bulk self-assembly of these ionic liquid crystals (ILCs) depends on the total number of side chains, yielding SmA and Lam_{Col} phases for ILCs with 2–3 chains and Col_{ro}, Col_h phases for ILCs with 3–6 chains. Thus, we demonstrated that thioethers are a useful design tool for ILCs with tailored properties.

Introduction

The combination of liquid crystalline materials with dye properties leads to highly attractive hybrid materials with unique self-assembly behavior and physical properties, which are suitable for a broad variety of applications ranging from non-linear optics,[1] photoresponsive and photoalignable materials,[2] dichroic, chromonic and laser dyes,[3] to electrochromic materials[4] and organic solar cells.[5] For many of these applications, solution processing and proper alignment of the liquid crystalline dyes are critical issues. In most cases, long alkoxy side chains attached to the mesogenic core increase the solubility in organic solvents and promote mesophase formation through van der Waals interactions. Otherwise, there is increasing experimental evidence from comparative studies that the grafting of alkylsulfanyl (thioether) side chains to the aromatic dye cores instead of alkoxy chains can have manifold beneficial effects on the performance of these liquid crystalline

materials. For example, it was reported that the replacement of alkoxy by alkylsulfanyl chains in non-mesomorphic benzo[1,2-b:4,5-b']bis[b]benzothiophenes led to increased melting points, antiperiplanar conformations and tighter packing in the solid state due to S···S interactions.[6] For H-bonded, mesomorphic benzoic acids phase transition temperatures of thioether-substituted derivatives were lower than the alkoxy analogues due to S···S interactions favoring smectic clusters in the nematic phase.[7] Rich polymorphism was observed for asymmetrically end-capped oligothiophenes upon attachment of thioethers.[8] Upon S/O replacement in the side chains of calamitic imidazolium ILCs, a pronounced decrease of the melting temperatures was detected, while clearing transitions remained constant or even increased, resulting in significantly broadened mesophase ranges.[9] For methylimidazolium ILCs the emergence of mesomorphic properties via the sulfur motif was reported.[10] Stabilization of mesophases was also found for columnar palladium complexes with dipicolinic acid-derived pincer ligands[11] and columnar crown ethers carrying thioethers instead of alkoxy side chains.[12] Furthermore, the S/O replacement led to a higher degree of order in columnar mesophases of 6-oxoverdazyl radicals.[13] In calamitic tolane derivatives, the S/O replacement resulted in a strong increase of the birefringence.[14]

Regarding the chromophoric part in liquid crystalline dyes, flavylium salts are very attractive. Flavylium salts, i.e. benzo-anellated 2-phenyloxonium salts belong to a large class of plant dyes (Figure 1).[15] Typical examples are malvin **1** and its aglycon malvidin.[15a] The presence of hydroxy groups in natural flavylium salts enables pH-dependent color shifts. The manifold substitution patterns found in nature lead to a large library of dyes[15] with many applications.[16] Besides their use as food colorants,[16d] synthetic flavylium salts have also been employed

[a] *J. A. Knöller, Dr. R. Forschner, Dr. W. Frey, Dr. J. Lang, A. Baro, Dr. A. Zens, Dr. B. Claasen, Prof. Dr. S. Laschat*
Institut für Organische Chemie
Universität Stuttgart (Germany)
E-mail: sabine.laschat@oc.uni-stuttgart.de
[b] *Prof. Dr. Y. Molard*
University of Rennes
CNRS, ISCR, UMR 6226, ScanMAT – UMS 2001, Rennes (France)
[c] *Prof. Dr. F. Giesselmann*
Institut für Physikalische Chemie
Universität Stuttgart, Germany
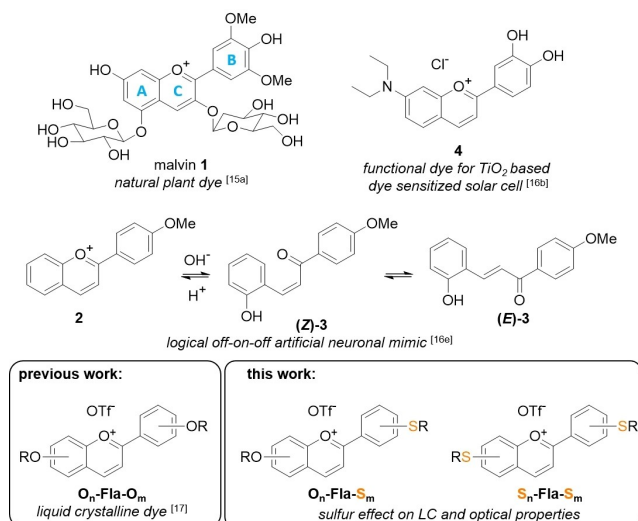
Figure 1. Flavylium salts found in nature (**1**),[15a] as sensitizers for organic solar cells (**4**)[16b] and as neuronal mimics (**2,3**)[16e] as well as liquid crystalline flavylium salts **O$_n$-Fla-O$_m$**[17] and new sulfur analogues **O$_n$-Fla-S$_m$**, **S$_n$-Fla-S$_m$**.

in more technical applications, such as logical "off-on-off" artificial neuronal mimics **2**, **3**[16e] and photosensitizers **4** for Grätzel-type solar cells.[16a–c,f]

We have recently developed flavylium-based[17] ionic liquid crystals[18] (ILCs) **O$_n$-Fla-O$_m$** (R=H, alkyl), which combine the birefringence and self-assembly of thermotropic neutral liquid crystals with the electrostatic interactions and tunability of polarity and solubility characteristic of ionic liquids as well as the absorption and emission characteristics of the flavylium chromophore (Figure 1). As our previous work emphasized the vital role of the substitution pattern on the mesomorphic properties of the flavylium ILCs, we were curious to highlight to what extent grafting of alkylsulfanyl side chains to the flavylium A and B rings (Figure 1) might affect the polymorphism, as well as the optical properties. Kaszynski[19] and our group[12] reported independently, that the attachment of thioethers to columnar mesogens increased the temperature range and enabled room temperature mesomorphism. These results motivated us to explore both thioether-substituted flavylium salts **O$_n$-Fla-S$_m$** carrying thioethers only at the B-ring and flavylium salts **S$_n$-Fla-S$_m$** carrying thioethers at both A and B ring. Solution NMR and X-ray diffraction studies were performed to gain insight into their self-assembly. As detailed below in the current manuscript, we report that the position of the thioether, i.e. A vs. B ring has a major impact on the self-assembly in solution and bulk state.
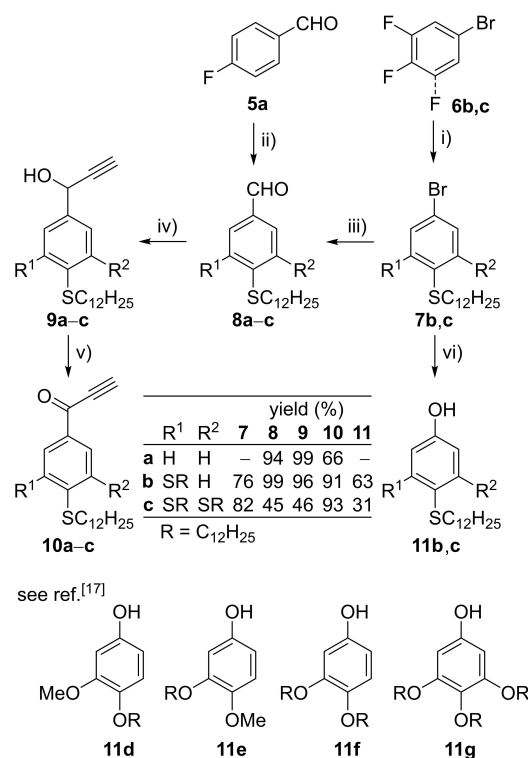
Results and Discussion

Synthesis of Thioether-Substituted Flavylium ILCs

In order to access the two libraries of flavylium ILCs **O$_n$-Fla-S$_m$** carrying alkoxy chains on the A ring and alkylsulfanyl chains on the B ring and flavylium ILCs **S$_n$-Fla-S$_m$** carrying alkylsulfanyl

side chains on both A and B ring, the previously described strategy by Chassaing was employed, where the flavylium core is generated by acid-mediated cyclocondensation of phenols and propargylic ketones.[17,20] As shown in Scheme 1, 4-fluorobenzaldehyde **5a** was treated with dodecanethiol in the presence of Na$_2$CO$_3$ adapting a procedure of Prasad[21] yielding **8a** in 94%. The corresponding aldehydes **8b,c** with two and three alkylsulfanyl chains were prepared according to Jankowiak[19] from known bromides **7b,c**[19] by formylation with nBuLi, DMF to give **8b** in 76% and **8c** in 82% respectively.

By following the protocol by Chassaing[20], the aldehydes **8a–c** were reacted with ethynyl magnesium bromide in THF to give the secondary propargylic alcohols **9a–c**, which were submitted to IBX oxidation to the ketones **10a–c** in 46–99% (over 2 steps). In order to obtain the required phenols **11b,c**, bis- and trisdodecyloxysulfanylphenylbromides **7b,c**[19] were treated with LiOH in DMSO / H$_2$O (4:1) in the presence of 10 mol% of Cu(acac)$_2$ and 10 mol% of BHMPO using the method by Ma[22] to yield **11b,c** in 63% and 31% respectively.

With the desired phenols **11b–g** including the known bis- or trisalkoxy-substituted phenols **11d–g** and the propargylic ketones **10a–c** at hand, the flavylium salts **O$_n$-Fla-S$_m$**, **S$_n$-Fla-S$_m$** were obtained by stirring a solution of the former in EtOAc in the presence of 2–4 equiv. of trifluoromethansulfonic acid for 24 h at room temperature and twofold recrystallization from EtOAc, which provided the mixed flavylium triflates **O$_n$-Fla-S$_m$** in

	R^1	R^2	yield (%)				
			7	**8**	**9**	**10**	**11**
a	H	H	–	94	99	66	–
b	SR	H	76	99	96	91	63
c	SR	SR	82	45	46	93	31

R = C$_{12}$H$_{25}$

Scheme 1. i) NaH, C$_{12}$H$_{25}$SH, DMSO, THF, 20°C, 4 h, 60°C, 6 h; ii) Na$_2$CO$_3$, C$_{12}$H$_{25}$SH, abs. DMSO, 160°C, 1 d; iii) 1) n-BuLi, abs. THF, −78°C, 2 h, 2) DMF, 1 h; iv) HCCMgBr, abs. THF, rt, 4 h; v) IBX, EtOAc, 80°C, 16 h; vi) H$_2$O$_2$, H$_2$SO$_4$, CHCl$_3$, MeOH, 16 h; vii) Cu(acac)$_2$ (10 mol%), BHMPO (10 mol%), LiOH•H$_2$O, DMSO/H$_2$O (4:1), 120°C, 6 d; * The alkoxy derivatives **10d–g** were prepared according to literature procedures.[17]

ChemPhysChem

Research Article
doi.org/10.1002/cphc.202200154

**Chemistry
Europe**

European Chemical
Societies Publishing

47–83%, except for compounds O_3-**Fla-S**$_1$, O_3-**Fla-S**$_3$, which were isolated in lower yields of 19% and 13% respectively (Scheme 2). In general, yields of thioether-substituted flavylium triflates S_n-**Fla-S**$_m$ were lower (11 – 32%) as compared to flavylium triflates O_n-**Fla-S**$_m$ with mixed alkoxy and thioether chains due to tedious purification requiring multiple recrystallization.

Fortunately, we were able to confirm the structure of O_1-**V-Fla-S**$_1$ via single crystal Xray diffraction, revealing the absence of any S,S interaction in the solid state (for details see Supporting Information, Figure S1).[23] Noteworthy, O_1-**V-Fla-S**$_1$ formed columnar stacks with antiparallel orientation of neighboring flavylium ions and resulting in π-π stacking of the pyrylium cores with a distance of 3.50 Å, which is similar to the solid-state structure of the known alkoxy derivative O_1-**V-Fla-O**$_1$.[17]

NMR Spectroscopic Studies on O_1-iV-Fla-S_3

Based on the known propensity of flavylium salts to form dimers and higher aggregates in solution resulting from strong intermolecular H-bonds (in the presence of free OH groups), anion-π, π-π and electrostatic interactions[15] standard 1D ^{1}H NMR experiments for characterization of flavylium salts O_n-**Fla**-
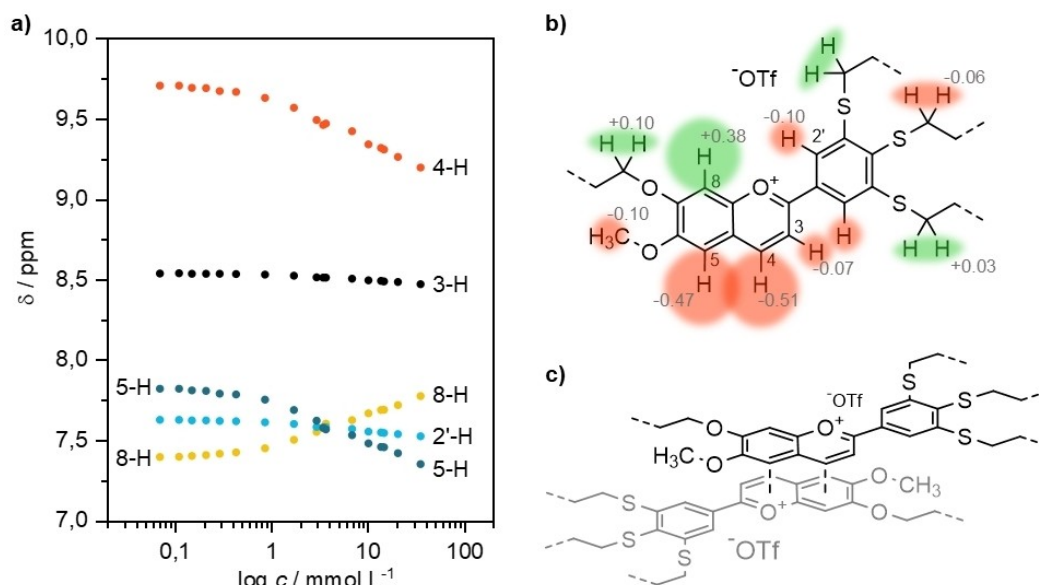
S_m, S_n-**Fla-S**$_m$ were performed with dilute solutions (concentration ≤ 3.4 mM) in CDCl$_3$. All spectra were well resolved and showed sharp NMR signals except for the ^{1}H NMR spectrum of compound O_1-**iV-Fla-S**$_3$, which exhibited significant line-broadening effects, even at low concentrations. To understand the observed behavior of this amphiphilic thioether-substituted flavylium salt, the aggregation of O_1-**iV-Fla-S**$_3$ in solution was studied by acquisition of concentration-dependent ^{1}H NMR spectra. With increasing concentration (concentration range: 0.07–14.7 mM) both up- and downfield shifts and broadening of some signals were observed (for details, see the Supporting Information, Figure S2), while other signals remained unaffected. The chemical shifts δ of diagnostic protons were plotted versus the concentration (Figure 2a), which revealed that 4-H, 5-H and 8-H of the benzopyrylium scaffold, i.e. the AC rings showed strong shifts ($\Delta\delta > 0.38$ ppm) (Figure 2b), whereas only minor effects ($\Delta\delta < 0.10$ ppm) were observed for 3-H, 2'-H, OCH$_2$, SCH$_2$. From these differences in $\Delta\delta$ values and their relative signs (i.e. upfield or downfield shift) and the fact that an upfield (downfield) shift is caused by increased shielding (deshielding) of a proton, a packing model can be proposed. As outlined in Figure 2c benzopyrylium AC units form the center of vertical aggregates, so called H-aggregates[24] with an antiparallel orientation of two neighboring AC rings within the columnar aggregate. Thus, 5-H and 4-H experience an upfield shift when oligomerization takes place, since both come to rest over the partially, negatively charged oxonium ion and the C-8 atom respectively (for charge distribution calculated via DFT, see Supporting Information, Figure S4). Additionally, by interacting with each other the 4-H and 8-H level out their strong differences in chemical shifts with increasing concentration. This packing model is supported by the X-ray crystallographic data of O_1-**V-Fla-S**$_1$ (Figure S1) and agrees well with experimental data for the oxygen-analogue O_1-**V-Fla-O**$_1$[17] and other flavylium salts in solid state and solution.[15]

To get a more detailed insight into the aggregation of O_1-**iV-Fla-S**$_3$, diffusion ordered NMR spectra (DOSY) were carried out.[25] Here, molecules are spatially labeled by use of field gradients. If they move during a following diffusion time, their position can be decoded by a second gradient. The measured signal is the integral over the whole sample volume, and it is attenuated depending on the diffusion coefficients of the analyte, the diffusion time and the gradient strength and length. The result is a "two-dimensional" NMR spectrum in which ^{1}H NMR spectrum of the sample is represented in F2 and the components are ordered in F1 with respect to their diffusion coefficients.

The experiments were performed with different concentrations of O_1-**iV-Fla-S**$_3$ (0.15–35.16 mM). The studies supported the presence of different oligomers in the given concentration range, since the signals of 4-H showed four different diffusion coefficients in the processed DOSY spectrum: 0.15 mM ($D = 7.41 \cdot 10^{-10}$ m^{2}s^{-1}), 0.15–1.47 mM ($D = 6.46 \cdot 10^{-10}$ m^{2}s^{-1}), 0.29–2.94 mM ($D = 5.62 \cdot 10^{-10}$ m^{2}s^{-1}) and 3.67–14.7 mM ($D = 4.90 \cdot 10^{-10}$ m^{2}s^{-1}) presumably caused by aggregates with different sizes (Figure S3).
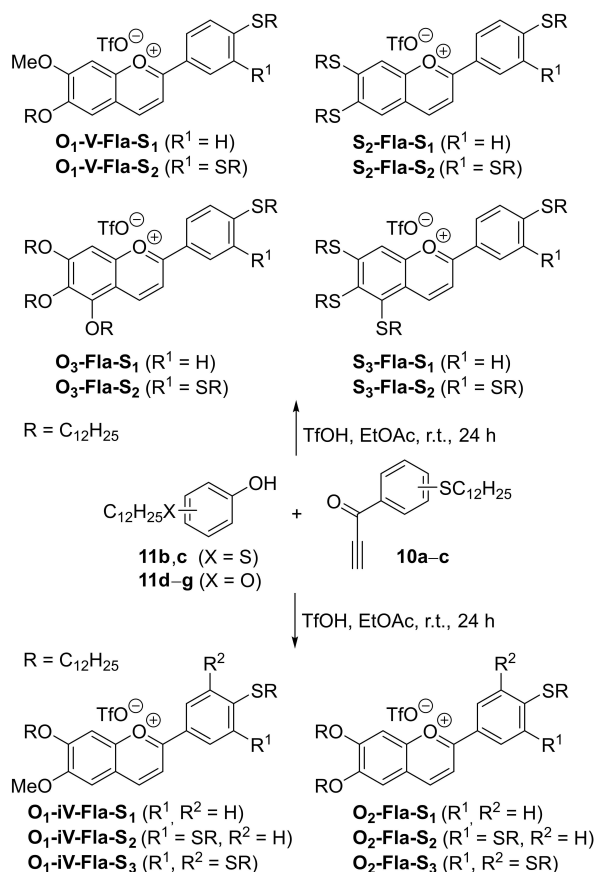
Scheme 2. Synthesis of the flavylium salts O_n-**Fla-S**$_m$ and S_n-**Fla-S**$_m$ from the ketones **10a-c** and phenols **11a-g** as well as substrate scope.

ChemPhysChem

Research Article
doi.org/10.1002/cphc.202200154

**Chemistry
Europe**
European Chemical
Societies Publishing

Figure 2. a) Chemical shift δ of the aromatic protons depending on the concentration. b) Change of the chemical shift $\Delta\delta$ from the lowest to the highest measured concentration (grey numbers, in ppm). c) Proposed packing model of a O_1-iV-**Fla**-S_3 dimer (alkyl chains are abbreviated by dashed lines).

It should be noted that Freitas reported diffusion and self-association constants of anthocyanins and flavylium/β-cyclodextrin inclusion complexes obtained by DOSY,[26] where the diffusion constants decrease with increasing aggregate size due to increasing hydrodynamic diameter. Although the experimentally determined diffusion constants were in a similar order of magnitude, direct comparison with flavylium salt O_1-iV-**Fla**-S_3 is not possible, because the applied solvents (D_2O/DMSO-D_6 vs. $CDCl_3$) and the investigated flavylium salts differ strongly in their polarity. Nevertheless, the NMR data suggests that the antiparallel columnar packing in the solid state is preserved to some extent in solution.

Mesomorphic Properties of Thioether-Substituted Flavylium ILCs

The mesomorphic properties were studied by optical polarizing microscopy (POM), differential scanning calorimetry (DSC) and X-ray diffraction (XRD). The results of the DSC measurements are summarized in Table S2. All thioether-substituted flavylium salts O_n-**Fla**-S_m, S_n-**Fla**-S_m were liquid crystalline except O_1-iV-**Fla**-S_1, S_3-**Fla**-S_1 and O_3-**Fla**-S_1. Furthermore, all liquid crystalline derivatives except O_2-**Fla**-S_2 and O_3-**Fla**-S_3 showed no signs of crystallization upon cooling but vitrified in a (metastable) glassy state preserving the mesophase textures.
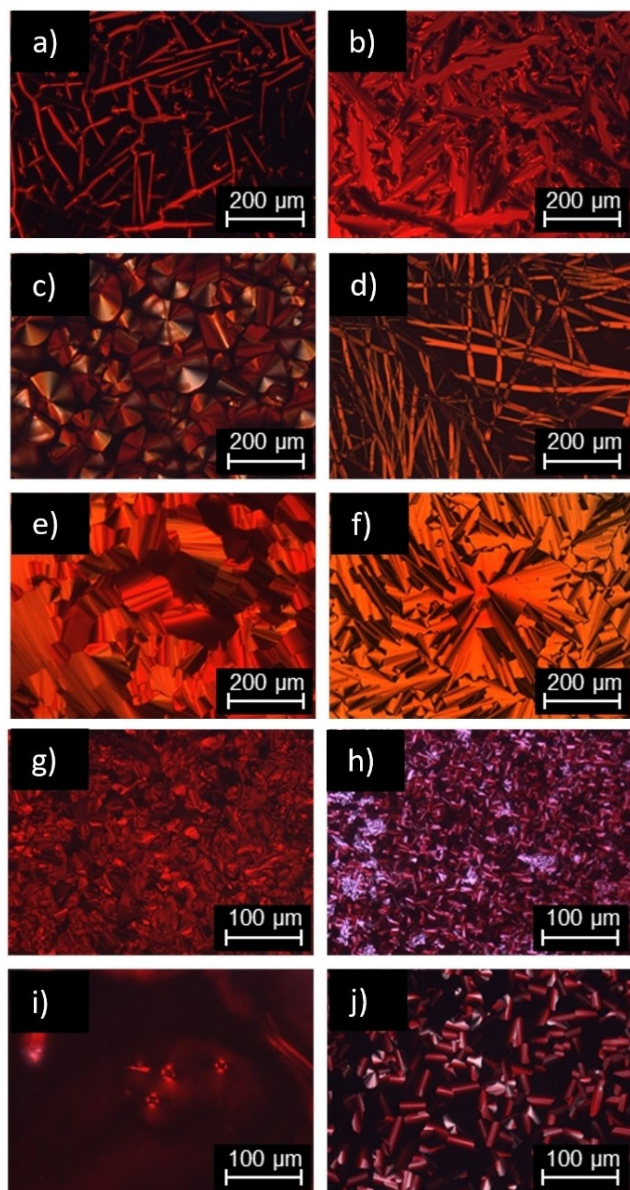
According to our investigations, the thioether-substituted flavylium ILCs could be grouped into two categories: (a) rod-shaped (calamitic) ILCs with up to 2 alkoxy chains on the A ring and only one thioether on the B ring showing lamellar mesophases only, and (b) disk-shaped (discotic) ILCs with 3–6 side chains in total and a minimum of 2 thioethers on the B ring displaying columnar mesophases.

ILCs O_1-V-**Fla**-S_1 and O_2-**Fla**-S_1 belonged to category (a). For example, upon cooling O_1-V-**Fla**-S_1 from the isotropic phase *Bâttonet* textures and large homeotropic areas were visible at 193 °C (Figure 3a), typical of a SmA phase. Upon further cooling, these textures changed into fan-like textures indicating a columnar phase (Figure 3b). Similar behavior was observed for O_2-**Fla**-S_1 (Figure S14a,b).

On the other hand, members of category (b) behaved differently under the POM. For example, O_1-iV-**Fla**-S_2 displayed pseudo-focal conic textures at 147 °C upon cooling (Figure 3c), while O_1-iV-**Fla**-S_3 showed filament-like textures at 150 °C (Figure 3d). Dendritic growth was detected for O_2-**Fla**-S_2 at 142 °C (Figure S14c) and fan-like textures with line defects and large homeotropic areas at 140 °C (Figure S14d). Fan-like textures were also observed for O_2-**Fla**-S_3 at 44 °C (Figure 3e) and O_3-**Fla**-S_3 at 146 °C (Figure 3f). According to the POM investigations, the fully thioether-substituted flavylium salts also belonged to category (b), showing pseudo-focal conic textures, e.g. for S_2-**Fla**-S_2 at 72 °C (Figure 3h) and S_3-**Fla**-S_2 at 22 °C (Figure 3j) with or without line defects and homeotropic regions upon cooling. The violet appearance of the textures is a result of the strong intrinsic color of the flavylium salts. Fan-shaped textures are common for smectic and columnar liquid crystals and further investigation via XRD was necessary to understand the mesomorphic behavior.

To fully assign the mesophase geometries, XRD studies were performed. All XRD data are summarized in Table 1. First, members of category (a) were examined. For O_1-V-**Fla**-S_1 (Figure 4a, at 130 °C) a sharp reflection in the small angle region at 31.65 Å and three reflections at 15.89 Å, 9.98 Å and 8.07 Å with smaller intensities were detected. These were assigned as (001), (002), (010) and (003) reflections of a lamellar columnar phase (Lam_{Col}) due to the perpendicular orientation of the (010)

ChemPhysChem

Research Article
doi.org/10.1002/cphc.202200154

**Chemistry
Europe**

European Chemical
Societies Publishing

Figure 3. POM micrographs of O_1-**V**-**Fla**-S_1 a) at 193 °C and b) at 178 °C. POM micrographs of c) O_1-**iV**-**Fla**-S_2 at 147 °C, d) O_1-**iV**-**Fla**-S_3 at 150 °C, e) O_2-**Fla**-S_3 at 44 °C and f) O_3-**Fla**-S_3 at 146 °C. POM micrographs of g) S_2-**Fla**-S_1 at 46 °C, h) S_2-**Fla**-S_2 at 72 °C, i) S_3-**Fla**-S_1 at −2 °C and j) S_3-**Fla**-S_3 at 22 °C. All pictures were taken between crossed polarizers upon cooling from the isotropic phase with a cooling rate of 5 K min⁻¹.

Figure 4. WAXS pattern (left) and diffractogram (right) and SAXS pattern (inset) of O_1-**V**-**Fla**-S_1 in a) the Lam_{Col} phase at 130 °C. b) the SmA phase at 190 °C. c) O_1-**V**-**Fla**-S_2 at 120 °C.

reflection regarding the other small angle reflections (Figure 4a). In the wide-angle section, a broad halo centered around 5.03 Å and an additional peak at 3.99 Å due to the π-π interactions were detected in the WAXS (Figure 4a). Upon increasing the temperature to 190 °C a distinct sharp reflection in the small angle region (Figure 4b), i.e. the (001) reflection of SmA layers together with a broad halo around 4.91 Å and a small π-π reflection peak at 3.94 Å were detected in the WAXS section. In a similar fashion, SAXS and WAXS data of O_2-**Fla**-S_1 indicated a Lam_{Col} phase at lower temperatures and a SmA phase at higher temperatures. The layer spacing in both

compounds is significantly smaller than the molecular length of about 42 Å, derived from the solid-state structure. This is due to a partial interdigitation of the alkyl chains, caused by increased effective cross sections by the anion of the charged ionic core, as previously reported.[17] The calamitic structure of the molecules belonging to category (a) is likely responsible for the formation of lamellar mesophases although a strong tendency for columnar stacking is already evident in the Lam_{Col} phases.

As mentioned above, members of category (b) exhibit different textures compared to category (a) under the POM. A typical diffraction pattern of O_1-**V**-**Fla**-S_2 is shown in Figure 4c. In the small angle regime at 120 °C a sharp intense and 5 weaker reflections were observed, which were indexed as (11) (20) (21) (12) (22) (32) reflections of a Col_{ro} phase. In the wide-angle regime, a broad halo centered around 4.62 Å and a second reflection at around 4.45 Å were detected. Fitting the wide angle regime (Figure 4c, dashed grey traces) revealed the later reflection consisting of the superposition of two reflections at 3.49 Å and 3.43 Å related to the anion distances (d_{anion}) and π-π interactions of the cationic cores (d_{core}) respectively.[17] In agreement with our previous report, alkyl chains and the cationic cores tilt out of the columnar plane in the Col_{ro} phase. While the alkyl tilt angle α_{alkyl} could be directly determined from the azimuthal angle of the halo of an oriented sample, the tilt

ChemPhysChem

Research Article
doi.org/10.1002/cphc.202200154

**Chemistry
Europe**

European Chemical
Societies Publishing

Table 1. XRD data of flavylium salts including the tilt angles α_{alkyl} and α_{core} for Col_{ro} phases.

Compound	Mesophase	Lattice parameters [Å]	d [Å][a]	Miller indices
O$_1$-V-Fla-S$_1$	SmA at 190 °C	–	29.53	(001)
			4.91	(halo)
			3.94	(π-π)
	Lam$_{Col}$ at 130 °C	–	31.65	(001)
			15.89 (15.83)	(002)
			9.98	(010)
			8.07 (7.91)	(003)
			5.03	(halo)
			3.99	(π-π)
O$_2$-Fla-S$_1$	SmA at 120 °C	–	29.33	(001)
			4.40	(halo)
	Lam$_{Col}$ at 90 °C	–	30.69	(001)
			15.42 (15.34)	(002)
			9.99 (10.23)	(003)
			9.56	(010)
			4.65	(halo)
O$_1$-V-Fla-S$_2$	Col$_{ro}$ at 120 °C $p2gg$ $\alpha_{alkyl}=36°$ $\alpha_{core}=(12°)$	$a=50.3$ $b=34.3$ $Z=4$	28.37	(11)
			25.17	(20)
			20.31 (20.30)	(21)
			16.34 (16.25)	(12)
			14.31 (14.19)	(22)
			12.06 (12.00)	(32)
			4.62	(halo)
			3.49	(anions)
			3.43	(π-π)
O$_1$-iV-Fla-S$_2$	Col$_{ro}$ at 100 °C $p2gg$ $\alpha_{alkyl}=37°$ $\alpha_{core}=(13°)$	$a=51.4$ $b=33.9$ $Z=4$	28.31	(11)
			25.71	(20)
			20.46 (20.49)	(21)
			16.21 (16.10)	(12)
			14.29 (14.15)	(22)
			12.12 (12.05)	(32)
			11.04 (11.10)	(13)
			10.28 (10.29)	(42)
			4.58	(halo)
			3.49	(anions)
			3.42	(π-π)
O$_1$-iV-Fla-S$_3$	Col$_{ro}$ at 100 °C $p2gg$ $\alpha_{alkyl}=37°$ $\alpha_{core}=34°$ (37°)	$a=53.3$ $b=33.4$ $Z=4$	28.31	(11)
			20.84	(21)
			16.64 (16.70)	(02)
			15.62 (15.69)	(31)
			14.33 (14.16)	(22)
			13.00 (13.33)	(40)
			12.35 (12.38)	(41)
			6.93 (6.98)	(π-π')
			4.57	(halo)
			4.20	(anions)
			3.49	(π-π)
O$_2$-Fla-S$_2$	Col$_{ho}$ at 135 °C $p6\,mm$	$a=30.4$ $Z=2$	26.35	(10)
			4.66	(halo)
			3.56	(π-π)
	Col$_{ro}$ at 100 °C $p2gg$ $\alpha_{alkyl}=45°$ $\alpha_{core}=(10°)$	$a=48.6$ $b=37.6$ $Z=4$	29.74	(11)
			24.31	(20)
			17.31 (17.53)	(12)
			15.31 (14.88)	(31)
			11.49 (11.57)	(41)
			4.61	(halo)
			3.62	(anions)
			3.56	(π-π)
O$_2$-Fla-S$_3$	Col$_{ho}$ at 100 °C	$a=26.6$ $Z=1$	23.03	(10)
			13.51 (13.30)	(11)
			4.46	(halo)
			3.62	(π-π)
O$_3$-Fla-S$_3$	Col$_{ho}$ at 100 °C	$a=25.6$ $Z=1$	22.04	(10)
			12.90 (12.81)	(11)
			11.07 (11.02)	(20)
			4.51	(halo)
			3.90	(π-π)
S$_2$-Fla-S$_1$	Col$_{ho}$ at 60 °C $p6\,mm$	$a=31.4$ $Z=2$	27.15	(10)
			15.82 (15.68)	(11)
			13.71 (13.57)	(20)

ChemPhysChem

Research Article
doi.org/10.1002/cphc.202200154

Chemistry
Europe
European Chemical
Societies Publishing

Table 1. continued

Compound	Mesophase	Lattice parameters [Å]	d [Å][a]	Miller indices
			4.62	(halo)
			3.62	(π-π)
S_2-**Fla**-S_2	Col_{ho}	$a = 27.1$	23.48	(10)
	at 90 °C	$Z = 1$	13.70 (13.56)	(11)
	$p6\,mm$		4.51	(halo)
			3.55	(π-π)
S_3-**Fla**-S_2	Col_{ho}	$a = 26.9$	23.49	(10)
	at 100 °C	$Z = 1$	13.56 (13.47)	(11)
	$p6\,mm$		4.40	(halo)
			3.49	(π-π)

[a] Calculated d values are given in parentheses.

angle of the core α_{core} was determined from the relation of d_{anion} and d_{core}: $\alpha_{core} = \cos^{-1}(d_{core}/ d_{anion})$.[17] For the Col_{ro} phase lattice parameters of $a = 50.3$ Å, $b = 34.3$ Å, $Z = 4$ and tilt angles of $\alpha_{alkyl} = 36$ ° and $\alpha_{core} = 12$ ° were calculated. The corresponding isovanilin-derived ILC O_1-**iV**-**Fla**-S_2 possessed similar phases and lattice parameters. For O_1-**iV**-**Fla**-S_3 the unit cell is slightly enlarged, despite the additional thioether side chain. However, the sterically more demanding B ring (as compared to O_1-**iV**-**Fla**-S_2) is compensated by a significant increase in the tilt of the aromatic core of 34°.

For O_2-**Fla**-S_2 a high temperature Col_{ho} phase with lattice parameter $a = 30.4$ Å and $Z = 2$ was deduced from the distinct (10) reflection in the SAXS, the broad halo around 4.66 Å and the small π-π reflection at 3.56 Å. At lower temperatures a Col_{ro} phase was found again. For the higher homologues O_2-**Fla**-S_3 and O_3-**Fla**-S_3 only Col_{ho} phases with lattice parameters of $a = 26.6$ Å and $a = 25.6$ Å respectively and $Z = 1$ were detected. It should be noted that lattice parameters of the hexagonal columnar mesophase decreased for these three ILCs despite the increased number of side chains. This can be rationalized as follows: In O_2-**Fla**-S_2, presumably two molecules form a discoid dimer whereas the increased B ring substitution in O_2-**Fla**-S_3, O_3-**Fla**-S_3 suppresses dimer formation. Consequently, when comparing O_2-**Fla**-S_2 and O_2-**Fla**-S_3, the lattice parameter decreases from $a = 30.4$ Å to $a = 26.6$ Å as the number of molecules in a unit cell decreases from 2 to 1. At the same time, the density decreases from $\rho = 1.31$ g·cm³ to $\rho = 0.99$ g·cm³ presumably due to a decreased space filling of the monomeric discoid O_2-**Fla**-S_3 compared to the dimeric discoid in O_3-**Fla**-S_3. Compared to O_2-**Fla**-S_3, the additional alkoxy chain in O_3-**Fla**-S_3 likely results in an increased space filling and thus in a smaller lattice parameter and an increased density of $a = 25.6$ Å and $\rho = 1.13$ g·cm³. Similar behavior was found for the series S_2-**Fla**-S_1, S_2-**Fla**-S_2 and S_3-**Fla**-S_2 (see Supporting Information, Table S3).

A similar packing behavior was found for fully thioether-substituted ILCs S_2-**Fla**-S_1, S_2-**Fla**-S_2, S_3-**Fla**-S_2. XRD results of S_2-**Fla**-S_1 confirmed a monotropic Col_{ho} phase. The lattice parameter of $a = 31.4$ Å indicated, that two flavylium ions form a discoid. Assuming an anti-parallel stacking of the flavylium cation in the Lam_{Col} phase, the increased steric demand of the sulfur atoms should disfavor this packing pattern, leading to reduced intermolecular interactions. As a result, rotation of the mesogens along the short molecular axis is less hindered, which

leads to a more disc-like appearance, thus promoting a columnar mesophase. Since 3 side chains are not sufficient to stabilize this phase, the mesogenic building block is a disk-like dimer with 6 side chains in total. According to the XRD data of S_2-**Fla**-S_2 and S_3-**Fla**-S_2 a Col_{ho} phase containing one flavylium salt per discoid was assigned in both cases (Table 1). The decreased intermolecular interactions of S_2-**Fla**-S_2 resulted in the Col_{ho} mesophase rather than a Col_{ro} mesophase as seen in O_2-**Fla**-O_2[17] and O_2-**Fla**-S_2, requiring stronger interactions to propagate the tilt of the columns. Evidently, molecules belonging to category exhibit columnar mesophases, which can be rationalized by the discotic geometry of derivatives with 2 or 3 thioethers tethered to the B ring.

The XRD results revealed the influence of the molecular structure on the mesophase geometry. Whereas calamitic ILCs (type A) such as O_1-**V**-**Fla**-S_1, O_2-**Fla**-S_1 consisting of a linear structure formed SmA or Lam_{Col} phases, even a slightly bend structure as in O_1-**iV**-**Fla**-S_1 or unsymmetrical compounds such as O_3-**Fla**-S_1 with large voids around the thioether side chain in the B ring supressed mesophase formation. On the other hand, with 2 thioethers at the B ring sufficient space filling could be achieved and Col_{ro} phases are favored for ILCs with up to 2 alkoxy chains at the A ring, e.g. O_2-**Fla**-S_2. The preference for Col_{ro} was also found, when the A ring carried only one alkoxy chain, as in O_1-**V**-**Fla**-S_2, O_1-**iV**-**Fla**-S_2 and O_1-**iV**-**Fla**-S_3 respectively. In contrast, ILCs with either 3 thioethers at the B ring or ≥ 2 thioethers at the A ring displayed Col_h phases. Thus, the increased steric bulk of the thioethers as compared to alkoxy chains minimized the free volume and resulted in improved temperature range and stability of the columnar mesophase as evident by comparison of O_2-**Fla**-S_2, O_2-**Fla**-S_3, S_2-**Fla**-S_2 in Figure 5. Members of discotic ILCs (type B) showed Col_{ro} phases mostly when alkoxy groups are grafted to the A ring, while Col_h phases were observed for derivatives with thioethers at the B ring.

The results of our DSC measurements and phase assignments were summarized in Figure 5. We want to point out that the investigated flavylium salts often vitrify in a (metastable) glass in agreement with our POM measurements and no crystallization or glass transition was detected in the cooling runs (see Supporting Information, Figure S5–S7 and Table S2). However, most derivatives exhibit a melting transition in the 1st heating cycles indicating a crystalline phase at room temper-

ChemPhysChem

Research Article
doi.org/10.1002/cphc.202200154

**Chemistry
Europe**
European Chemical
Societies Publishing
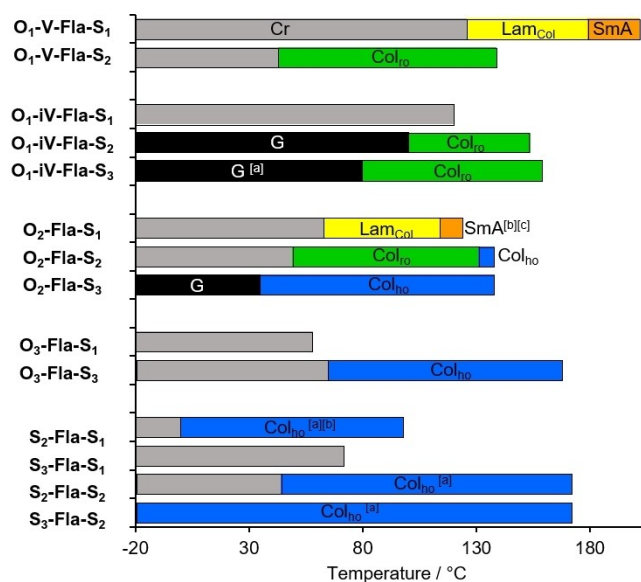
Figure 5. (Meso)phases and corresponding temperature ranges of the flavylium salts (temperatures determined from 1st heating cycles, rate = 10 K min^{-1}): Cr (crystalline), G (glass), SmA (smectic A), Lam$_{Col}$ (lamello-columnar), Col$_{ro}$ (ordered columnar rectangular), Col$_{ho}$ (ordered columnar hexagonal);[a] T_c/ T_G determined by slow cooling via POM;[b] monotropic behavior;[c] SmA – Lam$_{Col}$ transition determined from 1st cooling cycle.

ature. Furthermore, derivatives with melting or clearing points above 150 °C gave no reproducible DSC data indicating thermal decomposition. We therefore decided to investigate transition temperatures from the 1st heating cycles. The results of our DSC measurements and phase assignments were summarized in Figure 5 and allowed us to investigate the influence of substitution patterns on the mesomorphic properties.

Depending on the substitution pattern of the A ring, the following trends were observed. For flavylium salts O_1-**V-Fla-S$_m$** with one alkoxy chain at the A ring melting and clearing temperatures decreased upon increasing the number of thioethers m at the B ring. Furthermore, the phase type changed from Lam$_{Col}$, SmA for O_1-**V-Fla-S$_1$** to Col$_{ro}$ for O_1-**V-Fla-S$_2$**.

In contrast, in the series of regioisomeric flavylium salts O_1-**iV-Fla-S$_m$** clearing temperatures increased with larger m. Moreover, grafting of additional thioethers to the B ring induced a Col$_{ro}$ phase in O_1-**iV-Fla-S$_2$** and increased phase widths and stability in O_1-**V-Fla-S$_3$**.

Flavylium salts O_2-**Fla-S$_m$** with two alkoxy groups at the A ring displayed higher clearing temperatures respectively, upon increasing m. Within the series phase types changed from Lam$_{Col}$, SmA (for O_2-**Fla-S$_1$**) to Col$_{ro}$, Col$_{ho}$ (for O_2-**Fla-S$_2$**) and Col$_{ho}$ (for O_2-**Fla-S$_3$**), while simultaneously temperature range and phase stability increased.

On the other hand, flavylium salts O_3-**Fla-S$_m$** carrying three alkoxy chains at the A ring showed a slight increase of melting transitions but a very pronounced increase of clearing temperatures upon increasing m, resulting in a broad Col$_{ho}$ phase for O_3-**Fla-S$_3$** in contrast to the non-mesomorphic O_3-**Fla-S$_1$**.

When the A ring carried thioether chains, e.g in flavylium salts S_2-**Fla-S$_m$**, increased melting and clearing temperatures were observed with larger m. Upon comparison of S_2-**Fla-S$_1$** with S_2-**Fla-S$_2$**, the two thioethers at both A and B ring in the latter case improved the overall molecular symmetry and thus increased the stability of the Col$_{ho}$ phase. The beneficial effect of molecular symmetry and improved space filling on the mesophase stability is also visible for S_3-**Fla-S$_2$** with a broad Col$_{ho}$ phase and its non-mesomorphic counterpart S_3-**Fla-S$_1$**.

Comparison of thioether-substituted flavylium salts O_n-**Fla-S$_m$**, S_n-**Fla-S$_m$** with the corresponding alkoxy-substituted analogues O_n-**Fla-O$_m$**[17] revealed only a small influence of the thioether/ether replacement on the phase types, but a more pronounced effect on the phase stability. Two extreme cases are O_2-**Fla-O$_1$**, O_2-**Fla-S$_1$** showing both lamellar phases and O_3-**Fla-O$_1$**, O_3-**Fla-S$_1$** where the columnar mesomorphism is completely lost in the sulfur case (for further details, see Supporting Information, Figures S12, S13). The number of side chains and substitution pattern determines the overall molecular geometry and thus the phase type (vide infra). With 2–3 side chains at the B ring columnar phases are exclusively formed. Unsymmetrical members with alkoxy chains at the A ring and thioethers at the B ring displayed Col$_{ro}$ phases, while the correponding ILCs with thioethers at both A and B ring displayed Col$_h$ phases. Thioether/ether replacement decreased the columnar phase stability, presumably due to less efficient packing of the bulkier thioethers and the absence of S—S interactions. However, for symmetrical derivatives S_2-**Fla-S$_2$**, S_3-**Fla-S$_2$** Col$_h$ phases were much broader and more stable as compared to the O-analogues.

**Linear Optical Properties of Thioether-Substituted Flavylium ILCs**

All flavylium salts showed bright orange to purple colors in both solid state and solution and were thus investigated via UVVis and fluorescence spectroscopy in CHCl$_3$ solution. The lowest energy absorption bands (λ_{max} and ε) are summarized in Table 2 and selected spectra are shown in Figure 6. For example, vanillin-derivative O_1-**V-Fla-S$_1$** decorated with one alkoxy chain at the A ring and one alkylsulfanyl chain at the B ring displayed three weak absorptions in the UV-range (268 nm, 313 nm, 371 nm) and a strong absorption band in the visible region at 510 nm. Absorption maxima and extinction coefficients changed only marginally when the number of alkoxy chains n in the A ring increased in the series O_1-**V-Fla-S$_1$**, O_2-**Fla-S$_1$** and O_3-**Fla-S$_1$** while keeping the B ring pattern constant (Figure 6a). The same trend was observed within the series of O_n-**Fla-S$_2$** and O_n-**Fla-S$_3$** (Figure S15).

In contrast, when the A ring substitution was kept constant and the number of thioethers at the B ring increased, a distinct change of the absorption properties was detected. Within the series O_2-**Fla-S$_1$**, O_2-**Fla-S$_2$**, O_2-**Fla-S$_3$** ε values decreased. A bathochromic shift of 34 cm^{-1} was observed for O_2-**Fla-S$_2$** as compared to O_2-**Fla-S$_1$** (λ_{max} = 509 nm), while O_2-**Fla-S$_3$** displayed a hypsochromic shift of 89 cm^{-1}. The auxochromic effect

ChemPhysChem

Research Article
doi.org/10.1002/cphc.202200154

**Chemistry
Europe**

European Chemical
Societies Publishing

Table 2. Photophysical data of thioether-substituted flavylium salts O_n-**Fla**-S_m and S_n-**Fla**-S_m.

Compound	λ_{max} (ε) [nm (10^4 L mol^{-1} cm^{-1})][a]	λ_{em} (Φ) [nm (a.u.)][b]
O_1-V-Fla-S_1	510 (6.0)	571 (0.84)
O_1-V-Fla-S_2	518 (5.0)	–
O_1-iV-Fla-S_1	509 (4.9)	571 (-)
O_1-iV-Fla-S_2	518 (4.7)	–
O_1-iV-Fla-S_3	487 (2.8)	–
O_2-Fla-S_1	510 (6.5)	571 (0.86)
O_2-Fla-S_2	518 (5.3)	–
O_2-Fla-S_3	487 (3.0)	–
O_3-Fla-S_1	513 (5.8)	–
O_3-Fla-S_3	488 (2.8)	–
S_2-Fla-S_1	552 (9.8)	602 (<0.01)
S_2-Fla-S_2	571 (4.6)	–
S_3-Fla-S_1	567 (5.0)	–
S_3-Fla-S_2	575 (6.7)	–

[a] measured in CHCl$_3$ (c = $2 \cdot 10^{-5}$ L^{-1}), ε determined from 5 different concentrations; [b] measured in degassed CHCl$_3$ (c = $2 \cdot 10^{-5}$ L^{-1}), λ_{ex} = 510 nm, Φ measured with a calibrated integration sphere.
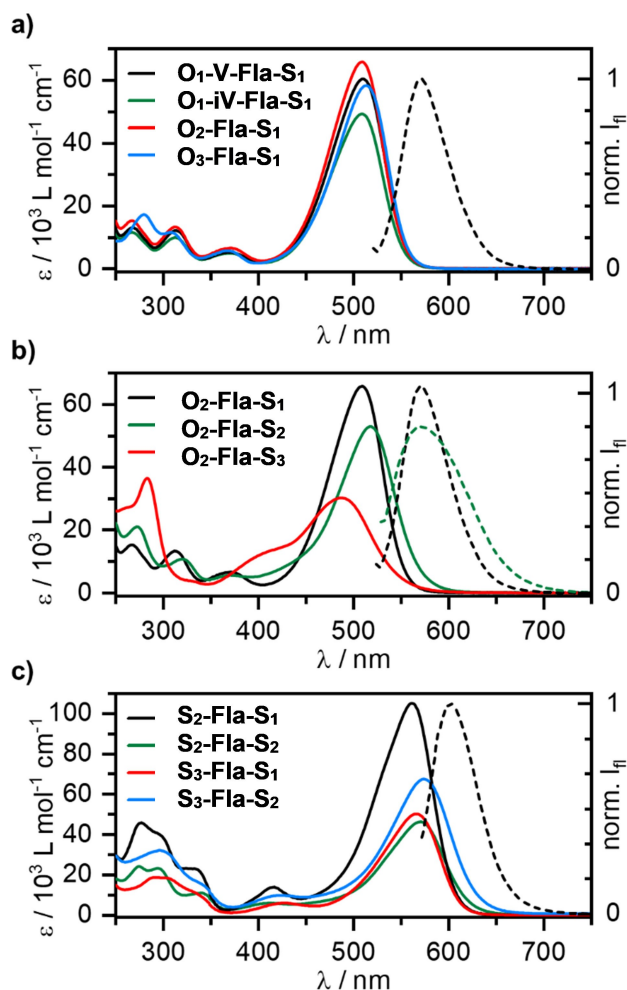
Figure 6. Absorption (solid lines) and, if applicable, emission (dashed lines) spectra of a) the series O_n-**Fla**-S_1, b) the series O_2-**Fla**-S_m and c) the series S_n-**Fla**-S_m recorded in CHCl$_3$ (c = $2 \cdot 10^{-5}$ mol L^{-1}, λ_{ex} = 510 nm).

ochromically shifted absorption bands (552–575 nm) (Figure 6c) compared to the analogues O_n-**Fla**-S_m.

Albeit most flavylium salts prepared in this work being non-emissive, the three derivatives O_1-**V-Fla**-S_1, O_1-**iV-Fla**-S_1 (Figure 6a) and O_2-**Fla**-S_1 (Figure 6b) exhibited bright emission (λ_{em} = 571 nm) upon irradiation in CHCl$_3$ solution. This is in accordance with the related alkoxy flavylium salts O_1-**Fla**-O_1, where decoration of the B ring with more than one substituent increased the rotational freedom of the peripheral phenyl ring and thereby partially or fully inhibited emission.[17]

The slightly lower quantum yields of O_1-**V-Fla**-S_1, O_1-**iV-Fla**-S_1 and O_2-**Fla**-S_1 compared to their alkoxy analogues[17] might be due to the decreased contribution of the flat Lewis structure with C=C double bond between A and C ring, resulting from the smaller electron-donating +M effect and less efficient orbital interaction of the larger thioethers as compared to the alkoxy chains.[17] It should be noted, that no evidence for side chains intercalating between the π-systems, as recently reported by Douce for luminescent naphthalene imidazolium ILCs,[27] could be found in our case. Additionally, the heavy atom effect[28] of the sulfur might be responsible for the experimental results. The unfavourable influence of sulfur-containing side chains on the luminescence was even more pronounced, when both A and B rings carried thioethers. For example, compound S_2-**Fla**-S_1 (λ_{em} = 602 nm, Figure 10c) was the only emitting compound of the series S_n-**Fla**-S_m with a very low quantum yield < 0.01. The rate of nonradiative relaxation usually increases with decreasing energy difference between S_1 and S_0 simply owing an improved overlap of higher vibrationally excited states in S_0 and the zeroth vibrational state in S_1 facilitating vibrational decay. This effect is commonly referred to as energy gap law[29] and might, in addition to the even more pronounced heavy atom effect, be responsible for the (almost) non-emissive behavior of the series S_n-**Fla**-S_m.

of the thioethers was even more pronounced for the fully thioether-functionalized compounds S_n-**Fla**-S_m resulting in bath-

ChemPhysChem

Research Article
doi.org/10.1002/cphc.202200154

**Chemistry
Europe**
European Chemical
Societies Publishing

Conclusions

In this work we have probed the self-assembly of ILCs based on flavylium salts with alkoxy side chains on the A ring and thioethers on the B ring (O_n-**Fla**-S_m series), as well as thioethers on both A and B ring (S_n-**Fla**-S_m series) and compared them with the corresponding known O-analogues O_n-**Fla**-O_m,[17] carrying alkoxy chains on both A and B ring respectively.

In solution isovanillin-derived ILC O_1-**iV-Fla**-S_3 with one alkoxy chain on the A ring and three thioethers on the B ring showed dynamic behaviour on the NMR time scale. DOSY experiments revealed four different diffusion constants (4.9–$7.4 \cdot 10^{-10}\ m^2 s^{-1}$) caused by columnar aggregates of different sizes.

UV/Vis spectra of the flavylium salts in solution showed an auxochromic effect of thioethers in O_n-**Fla**-S_m, S_n-**Fla**-S_m as compared to O-analogues O_n-**Fla**-O_m. Among the studied flavylium salts only O_1-**V-Fla**-S_1, O_1-**iV-Fla**-S_1 and O_2-**Fla**-S_1 with one thioether in the B ring displayed a bright green emission with high quantum yields ($\Phi = 84\%$), while S_2-**Fla**-S_1 showed only a weak yellow emission ($\Phi < 1\%$). All other derivatives seem to favor conformations with a high degree of rotational freedom and thus a strong tendency for thermal deactivation. Presumably, formation of H-aggregates also contributes to fluorescence quenching.

In the bulk state, POM, DSC and XRD provided insight into the liquid crystalline self-assembly. In the O_n-**Fla**-S_m series the presence of thioethers in the B ring led to lower clearing points except for O_1-**iV-Fla**-S_3, which has a higher clearing temperature as compared to the O-analogue O_1-**iV-Fla**-O_1.

For mixed O/S-substituted ILCs, the mesophase type changed upon increasing the number of thioethers on the B ring from SmA, Lam_{Col} for calamitic ILCs carrying one thioether at the B ring and 1–2 alkoxy chains at the A ring, via Col_{ro} for discotic ILCs carrying 2–3 thioethers at the B ring and 1–2 alkoxy chains at the A ring to Col_{ho} for discotic ILCs carring up to 3 thioethers at both A and B rings. The replacement of O by S in the side chain resulted in most cases in decreased mesophase stability and temperature range without affecting the phase type, in particular for ILCs carrying alkoxy chains at the A ring and thioethers at the B ring. However, for fully thioether-substituted derivatives S_2-**Fla**-S_1, S_2-**Fla**-S_2, S_3-**Fla**-S_2 a significant stabilization of the Col_{ho} phase was observed. Moreover, for S_2-**Fla**-S_1 the bulkiness of the thioethers induced a switch of the phase type from Lam_{Col} / SmA found for the alkoxy analogues O_2-**Fla**-S_1, O_2-**Fla**-O_1 to Col_{ho}.

Thus, the attachment of thioethers rather than alkoxy side chains to flavylium ILCs strongly favors columnar aggregates both in solution as well as in the bulk state. Future work must demonstrate whether this O/S replacement-induced change of mesophase type can be applied to other classes of ILCs as well.

Acknowledgements

Conflict of Interest

There are no conflicts to declare.

Data Availability Statement

The data that supports the findings of this study are available in the supplementary material of this article.

[1] N. V. Tabiryan, I.-C. Khoo, *Handbook of Liquid Crystals*, J. W. Goodby, P. J. Collings, T. Kato, C. Tschierske, H. Gleeson, P. Raynes (eds.), 2nd ed., Wiley-VCH, Weinheim, **2014**, *vol. 8*, 453–473.

[2] T. Seki, N. Kawatsuki, M. Kondo, *Handbook of Liquid Crystals*, J. W. Goodby, P. J. Collings, T. Kato, C. Tschierske, H. Gleeson, P. Raynes (eds.), 2nd ed., Wiley-VCH, Weinheim, **2014**, *vol. 8*, 539–579.

[3] S. J. Cowling, *Handbook of Liquid Crystals*, J. W. Goodby, P. J. Collings, T. Kato, C. Tschierske, H. Gleeson, P. Raynes (eds.), 2nd ed., Wiley-VCH, Weinheim, **2014**, *vol. 8*, 581–625.

[4] K. Isoda, T. Yasuda, M. Funahashi, T. Kato, *Handbook of Liquid Crystals*, J. W. Goodby, P. J. Collings, T. Kato, C. Tschierske, H. Gleeson, P. Raynes (eds.), 2nd ed., Wiley-VCH, Weinheim, **2014**, *vol. 8*, 709–725.

[5] a) F. Würthner, K. Meerholz, *Chem. A Eur. J.* **2010**, *16*, 9366–9373; b) F. Würthner, *Acc. Chem. Res.* **2016**, *49*, 868–876.

[6] S. Riaz, M. Edgar, M. R. J. Elsegood, L. Horsburgh, S. J. Teat, T. G. Warwick, G. W. Weaver, *Cryst. Growth Des.* **2019**, *19*, 5237–5248.

[7] Y. Arakawa, Y. Sasaki, K. Igawa, H. Tsuji, *New J. Chem.* **2017**, *41*, 6514–6522.

[8] Q. Meng, X. H. Sun, Z. Lu, P. F. Xia, Z. Shi, D. Chen, M. S. Wong, S. Wakim, J. Lu, J. M. Baribeau, Y. Tao, *Chem. A Eur. J.* **2009**, *15*, 3474–3487.

[9] M. Mansueto, K. C. Kreß, S. Laschat, *Tetrahedron* **2014**, *70*, 6258–6264.

[10] S. T. Nestor, B. Heinrich, R. A. Sykora, X. Zhang, G. J. McManus, L. Douce, A. Mirjafari, *Tetrahedron* **2017**, *73*, 5456–5460.

[11] P. Espinet, E. García-Orodea, J. A. Miguel, *Inorg. Chem.* **2000**, *39*, 3645–3651.

[12] J. Kirres, K. Schmitt, I. Wurzbach, F. Giesselmann, S. Ludwigs, M. Ringenberg, A. Ruff, A. Baro, S. Laschat, *Org. Chem. Front.* **2017**, *4*, 790–803.

[13] A. Jankowiak, D. Pociecha, J. Szczytko, H. Monobe, P. Kaszyński, *Liq. Cryst.* **2014**, *41*, 385–392.

[14] a) N. J. Chothani, V. K. Akbari, P. S. Patel, K. C. Patel, *Mol. Cryst. Liq. Cryst.* **2016**, *631*, 31–46; b) Y. Arakawa, S. Kang, H. Tsuji, J. Watanabe, G. I. Konishi, *RSC Adv.* **2016**, *6*, 16568–16574; c) D. Węgłowska, P. Kula, J. Herman, *RSC Adv.* **2015**, *6*, 403–408; d) B. He, J. Dai, D. Zherebetskyy, T. L. Chen, B. A. Zhang, S. J. Teat, Q. Zhang, L. Wang, Y. Liu, *Chem. Sci.* **2015**, *6*, 3180–3186; e) J. Mack, N. Kobayashi, M. J. Stillman, *J. Inorg. Biochem.* **2010**, *104*, 310–317; f) Y. Morita, R. Ono, H. Okamoto, K. Kasatani, *Trans. Mater. Res. Soc. Japan* **2009**, *34*, 455–458; g) W. Su, Y. Zhang, C. Zhao, X. Li, J. Jiang, *ChemPhysChem* **2007**, *8*, 1857–1862; h) M. Hird, A. J. Seed, K. J. Toyne, J. W. Goodby, G. W. Gray, D. G. McDonnell, *J. Mater. Chem.* **1993**, *3*, 851–859; i) M. Charton, *J. Org. Chem.* **1978**, *43*, 3995–4001.

[15] a) F. Pina, M. J. Melo, C. A. T. Laia, A. J. Parola, J. C. Lima, *Chem. Soc. Rev.* **2012**, *41*, 869–908; b) F. Pina, V. Petrov, C. A. T. Laia, *Dyes Pigm.* **2012**, *92*, 877–889; c) T. Goto, T. Kondo, *Angew. Chem. Int. Ed. Engl.* **1991**, *30*, 17–33.

ChemPhysChem

Research Article
doi.org/10.1002/cphc.202200154

**Chemistry
Europe**
European Chemical
Societies Publishing

[16] a) B. A. Aguilar-Castillo, N. A. Sánchez-Bojorge, D. Chávez-Flores, A. A. Camacho-Dávila, E. Pasillas-Ornelas, L.-M. Rodríguez-Valdez, G. Zaragoza-Galán, *J. Mol. Struct.* **2018**, *1155*, 414–423; b) G. Calogero, I. Citro, G. Di Marco, S. Caramori, L. Casarin, C. A. Bignozzi, J. Avó, A. Jorge Parola, F. Pina, *Photochem. Photobiol. Sci.* **2017**, *16*, 1400–1414; c) G. Calogero, A. Sinopoli, I. Citro, G. Di Marco, V. Petrov, A. M. Diniz, A. J. Parola, F. Pina, *Photochem. Photobiol. Sci.* **2013**, *12*, 883–894; d) F. J. Francis, P. C. Markakis, *Critical Reviews in Food Science and Nutrition Food Colorants: Anthocyanins*, **2009**; e) F. Pina, M. J. Melo, M. Maestri, P. Passaniti, V. Balzani, *J. Am. Chem. Soc.* **2000**, *122*, 4496–4498; f) N. J. Cherepy, G. P. Smestad, M. Grätzel, J. Z. Zhang, *J. Phys. Chem. B* **1997**, *101*, 9342–9351.

[17] R. Forschner, J. Knelles, K. Bader, W. Frey, C. Müller, A. Köhn, Y. Molard, F. Giesselmann, S. Laschat, *Chem. Eur. J.* **2019**, 12966–12980.

[18] a) K. Goossens, K. Lava, C. W. Bielawski, K. Binnemans, *Chem. Rev.* **2016**, *116*, 4643–4807; b) Y. Ji, R. Shi, Y. Wang, G. Saielli, *J. Phys. Chem. B* **2013**, *117*, 1104–1109; c) S. Chen, S. H. Eichhorn, *Isr. J. Chem.* **2012**, *52*, 830–843; d) L. Douce, J. M. Suisse, D. Guillon, A. Taubert, *Liq. Cryst.* **2011**, *38*, 1653–1661; e) K. V. Axenov, S. Laschat, *Materials (Basel).* **2011**, *4*, 206–259; f) K. Binnemans, *Chem. Rev.* **2005**, *105*, 4148–4204; g) S. K. Pal, S. Kumar, in *Biosensors Nanotechnology*, ed. A. Tiwani, A. P. F. Turner, Scrivener Publishing, Berkeley, MA, 2014, pp. 267–314; h) N. Kapernaum, A. Lange, M. Ebert, M. A. Grunwald, C. Haege, S. Marino, A. Zens, A. Taubert, F. Giesselmann, S. Laschat, *ChemPlusChem* **2022**, *87*, e202100397.

[19] A. Jankowiak, Z. Débska, J. Romański, P. Kaszyński, *J. Sulfur Chem.* **2012**, *33*, 1–7.

[20] S. Chassaing, M. Kueny-Stotz, G. Isorez, R. Brouillard, *Eur. J. Org. Chem.* **2007**, *2007*, 2438–2448.

[21] Q. Zheng, G. S. He, P. N. Prasad, *J. Mater. Chem.* **2005**, *15*, 579–587.

[22] S. Xia, L. Gan, K. Wang, Z. Li, D. Ma, *J. Am. Chem. Soc.* **2016**, *138*, 13493–13496.

[23] CCDC 2155920 (**O₁-V-Fla-S₁**) contains the supplementary crystallographic data for this paper. The data is provided free of charge by The Cambridge Crystallographic Data Centre. For comparison see CCDC 1913060 (**O₁-V-Fla-O₁**) reported in ref. [17].

[24] N. C. Maiti, S. Mazumdar, N. Periasamy, *J. Phys. Chem. B* **1998**, *102*, 1528–1538.

[25] D. H. Wu, A. Chen, C. S. Johnson, *J. Magn. Reson. Ser. A* **1995**, *115*, 260–264.

[26] a) A. Fernandes, N. F. Brás, N. Mateus, V. De Freitas, *New J. Chem.* **2015**, *39*, 2602–2611; b) A. Fernandes, N. F. Brás, N. Mateus, V. De Freitas, *Langmuir* **2014**, *30*, 8516–8527.

[27] a) N. del Giudice, M. L'Her, E. Scrafton, Y. Atoini, G. Gentile, B. Heinrich, R. Berthiot, A. Aliprandi, L. Douce, *Eur. J. Org. Chem.* **2021**, 2091–2098; b) M. L'Her, Y. Atoini, J. Fouchet, B. Heinrich, N. Del-Gioudice, E. Scrafton, E. Bordes, L. Karmazin, L. Charbonniere, L. De Cola, L. Douce, *New J. Chem.* **2020**, *44*, 2669–2669; c) J. Fouchet, B. Heinrich, M. L'Her, E. Voirin, L. Karmazin, C. Bailly, R. Welter, A. Mirjafari, L. Douce, *New J. Chem.* **2018**, *42*, 10421–10431.

[28] K. Michael, *Discuss. Faraday Soc.* **1950**, *9*, 14–19.

[29] a) Y.-C. Wei, S. F. Wang, Y. Hu, L.-S. Liao, D.-G. Chen, K.-H. Chang, C.-W. Wang, S.-H. Liu, W.-H. Chan, J.-L. Liao, et al., *Nat. Photonics* **2020**, *14*, 570–577; b) S. H. Lin, *J. Chem. Phys.* **1970**, *53*, 3766–3767.